Applied Clay Science 216 (2022) 106356

Contents lists available at ScienceDirect

Applied Clay Science

journal homepage: www.elsevier.com/locate/clay

Sorption/desorption of Eu(III) on halloysite and kaolinite

Junming Zhou [a,b], Hongmei Liu [a], Dong Liu [a,*], Peng Yuan [a], Hongling Bu [c], Peixin Du [d], Wenxiao Fan [a,b], Mengyuan Li [a,b]

[a] CAS Key Laboratory of Mineralogy and Metallogeny / Guangdong Provincial Key Laboratory of Mineral Physics and Materials, Guangzhou Institute of Geochemistry, CAS Center for Excellence in Deep Earth Science, Chinese Academy of Sciences, Guangzhou 510640, China
[b] University of Chinese Academy of Sciences, Beijing 100049, China
[c] National Regional Joint Engineering Research Center for Soil Pollution Control and Remediation in South China, Guangdong Key Laboratory of Integrated Agro-environmental Pollution Control and Management, Guangdong Institute of Eco-Environmental Science & Technology, Guangdong Academy of Sciences, Guangzhou 510650, China
[d] State Key Laboratory of Lunar and Planetary Sciences, Macau University of Science and Technology, Macau, China

ARTICLE INFO

Keywords:
Eu
Sorption
Desorption
Halloysite
Kaolinite
Weathered crust elution-deposited rare earth ores

ABSTRACT

Weathered crust elution-deposited rare earth (WED-RE) ores are important rare earth element (REE) resources around the world. In these ores, the REE are believed to mainly exist as exchangeable REE(III) ions on the surfaces of clay minerals, such as tubular halloysite and platy kaolinite. However, the mechanisms underlying the sorption and desorption of REE(III) ions on clay minerals in the environment of weathered crusts remain ambiguous. In this study, the sorption/desorption characteristics of Eu(III) ions onto halloysite and kaolinite were investigated. The results revealed that Eu(III) was adsorbed onto both clay minerals through inner-sphere complexation and outer-sphere complexation, where the former was the primary sorption mechanism. Halloysite displayed a higher sorption capacity for Eu(III) than kaolinite in a weakly acidic environment (pH 4–6). The desorption efficiency increased with the increasing concentration of NH_4^+ ions. When the NH_4^+ concentration was 0.002 mol/L, which is similar to the typical cation concentration of groundwater/rainwater, the amount and rate of Eu(III) desorption from halloysite were lower than those from kaolinite. The desorption of Eu(III) ions from the two clay minerals is proposed to be governed by the attraction between the outer-sphere complexes and clay minerals when the NH_4^+ concentration is 0.002 mol/L. Therefore, halloysite has a higher sorption capacity and stronger retention capacity for Eu(III) than kaolinite, which suggests that halloysite may play a greater role in REE(III) enrichment in WED-RE ores than kaolinite owing to the similar chemical properties of REE(III) ions. The fundamental results obtained in this study afford new insights into the migration of REE and the role of clay minerals in REE enrichment during ore formation.

.

1. Introduction

Rare earth elements (REE) are crucial materials for manufacturing numerous high-tech products with diverse applications in medical, defense, aerospace, renewable energy, and automobile industries (McLellan et al., 2013; Dutta et al., 2016; Yin et al., 2017). The demand for REE has been increasing rapidly every year (Dutta et al., 2016), and approximately one-quarter of the global REE supply is derived from weathered crust elution-deposited rare earth (WED-RE) ores (Su, 2009; Li et al., 2017), which are also called ion adsorption deposits (IAD) (Estrade et al., 2019). In particular, over 80% of the supply of heavy rare earth elements (HREE), the most valuable and sought-after REE (Ram et al., 2019), is sourced from WED-RE ores (Li et al., 2017). Although the REE grade in WED-RE ores generally is relatively low (Tian et al., 2010; Chakhmouradian and Wall, 2012; Li et al., 2017), their accessibility by opencast working and facile extraction process through ion exchange (Chakhmouradian and Wall, 2012) make these ores play an important role in the global REE market.

WED-RE ores were commonly formed by the weathering of various bedrocks (Bao and Zhao, 2008), and the REE are predominantly present

* Corresponding author at: CAS Key Laboratory of Mineralogy and Metallogeny, Guangzhou Institute of Geochemistry, Chinese Academy of Sciences (CAS), Wushan, Guangzhou 510640, China.
E-mail address: liudong@gig.ac.cn (D. Liu).

https://doi.org/10.1016/j.clay.2021.106356
Received 14 August 2021; Received in revised form 26 October 2021; Accepted 13 November 2021
Available online 25 November 2021

as exchangeable ions (Chi and Tian, 2008; Tian et al., 2010; Xiao et al., 2016, 2017). These REE(III) ions are easily extracted by using various electrolyte solutions, such as NaCl, $(NH_4)_2SO_4$, and $MgCl_2$ (Moldoveanu and Papangelakis, 2013; Estrade et al., 2019; Borst et al., 2020). The minerals in WED-RE ores mainly include clay minerals and unweathered rock-forming minerals (e.g., quartz and feldspar). The occurrence of exchangeable REE(III) ions is associated with the abundant clay minerals in WED-RE ores (Bao and Zhao, 2008), in which the total REE concentration was more than twice that in their bulk samples (Liu et al., 2016a; Zhou et al., 2018). The clay minerals in WED-RE ores are primarily composed of tubular halloysite and platy kaolinite (Yang, 1987; Bao and Zhao, 2008; Chakhmouradian and Wall, 2012; Kynicky et al., 2012; Li et al., 2017; Ram et al., 2019). Compared to quartz and feldspar, halloysite and kaolinite exhibit large specific surface area (SSA) and high cation exchange capacity (CEC), which are beneficial for the sorption of REE(III) ions. Thus, these clay minerals are considered to be excellent carriers for the exchangeable REE(III) ions in WED-RE ores (Chakhmouradian and Wall, 2012).

The exchangeable REE(III) ions accumulate on clay minerals through sorption (Borst et al., 2020), which is proposed to be a key process in the formation of WED-RE ore. The REE(III) ions released from REE-bearing minerals undergoing chemical erosion subsequently migrate with the rainwater/groundwater (Nesbitt, 1979; Bao and Zhao, 2008; Sanematsu and Watanabe, 2016) and could be adsorbed on the clay minerals mainly through outer-sphere complexation (Yamaguchi et al., 2018; Borst et al., 2020). However, several cations in the rainwater/groundwater, such as Na^+, Mg^{2+}, and NH_4^+ (Huang et al., 2013; Zhang et al., 2015), can exchange with some of the REE(III) ions adsorbed on the surfaces of clay minerals (Moldoveanu and Papangelakis, 2013; Estrade et al., 2019; Borst et al., 2020), resulting in their desorption. As a result of this sorption and desorption of REE(III) ions on clay minerals, the REE concentrations vary with the depth in weathered crusts (Chi and Tian, 2008). Therefore, the enrichment of exchangeable REE(III) ions is governed by the processes of sorption and desorption (Chi and Tian, 2008; Tian et al., 2010).

Previous studies have investigated the sorption of REE(III) ions on halloysite and kaolinite through laboratory experiments (Coppin et al., 2002; Yang et al., 2019). The ionic strength of a liquid in the environment is believed to be a key factor influencing the fractionation of REE (III) ions during their sorption on clay minerals. In a high-ionic-strength environment (e.g., 0.5 mol/L $NaNO_3$), clay minerals (e.g., kaolinite, montmorillonite, and halloysite) favor the accumulation of HREE compared with light rare earth elements (LREE), due to the competitive sorption of Na^+ ions and its steric effect (Yang et al., 2019). However, in a low-ionic-strength environment (e.g., 0.01 mol/L), the influence of clay minerals on the fractionation of REE(III) ions is almost negligible (Yang et al., 2019). Because the total ionic concentration in rainwater/groundwater is typically very low (e.g., 0.002–0.004 mol/L) (Huang et al., 2013; Zhang et al., 2015; Estrade et al., 2019), the fractionation of REE(III) ions due to the sorption by clay minerals (i.e., halloysite and kaolinite) in weathered crusts could be negligible and their sorption characteristics should be very similar. On the other hand, the pH value affects the sorption coefficients of REE(III) ions on clay minerals, with the sorption capability increasing with increasing pH (Bradbury and Baeyens, 2002; Coppin et al., 2002; Yang et al., 2019). This phenomenon is associated with the surface properties of the clay minerals (e.g., the deprotonation of the surface hydroxyl groups as pH increases) (Bradbury and Baeyens, 2002; Tertre et al., 2006; Lu et al., 2016).

The surface reactions of clay minerals such as sorption processes, are determined by their surface properties and structure (Schoonheydt and Johnston, 2013; Matusik, 2016). Halloysite and kaolinite possess distinct morphologies and structures although both of them are kaolin-group minerals and have a similar chemical composition and layered structure composed of $AlO_2(OH)_4$ octahedral sheet and SiO_4 tetrahedral sheet (Joussein et al., 2005; Yuan et al., 2015). Ordinarily, kaolinite has a pseudohexagonal platy morphology with diameters ranging from submicron to several microns (Keller, 1978; Aparicio et al., 2009). In contrast, halloysite has a tubular morphology (Banfield and Eggleton, 1990; Li et al., 2019) with the particle length and width ranging widely from 0.02 to >30 μm and from 50 to 200 nm, respectively (Joussein et al., 2005). These differences in structure between tubular halloysite and platy kaolinite result in various sorption efficiencies for REE(III) ions (Yang et al., 2019). As speculated in previous studies, REE(III) ions are adsorbed onto clay minerals (e.g., halloysite, kaolinite, and montmorillonite) through inner-sphere complexation and/or outer-sphere complexation (Takahashi et al., 2000; Coppin et al., 2002; Yang et al., 2019). However, these experiments involved the co-sorption of 15 REE (III) ions (Coppin et al., 2002; Yang et al., 2019), which rendered it difficult to comprehensively characterize the individual elements using spectroscopic methods (e.g., X-ray photoelectron spectroscopy (XPS)) owing to their low sorption amounts. Therefore, the sorption mechanisms for the two clay minerals have not been well established to date.

In addition to sorption, desorption is another vital yet poorly characterized process underlying the formation of WED-RE ores. Due to the economic incentive, almost all of the previous studies focused on the extraction of REE(III) ions from the WED-RE ores, such as developing suitable extractants for REE(III) ions and optimizing the extraction processes. For example, several monovalent or divalent cations (e.g., NH_4^+, Na^+, and Mg^{2+}) have been investigated as efficient extractants for REE(III) ions (Moldoveanu and Papangelakis, 2013; Estrade et al., 2019), and the extraction efficiency of REE(III) has been reported to increase with increasing electrolyte solutions concentration (Moldoveanu and Papangelakis, 2012; Chen et al., 2020) and also changes with pH (Li, 2014; Xiao et al., 2015). However, the desorption characteristics and mechanism of REE(III) ions from halloysite and kaolinite remain far from understood.

In this study, Eu(III) ions were used as model REE(III) ions due to their similar chemical properties, such as their similar chemical species in the weakly acid and low ionic-strength aqueous solution (Bau, 1999). The sorption and desorption of Eu(III) ions onto halloysite and kaolinite were comprehensively characterized using inductively coupled plasma mass spectrometry (ICP-MS) and XPS. The results revealed the characteristics and reaction mechanisms of the sorption and desorption of Eu (III) ions by the clay minerals, which are very significant to understand the potential important role of halloysite and kaolinite in the REE(III) enrichment, the geochemical behaviors of REE(III) ions in the weathered crusts, and the formation of WED-RE ores.

2. Experimental

2.1. Sample characterization

The tubular halloysite (Hal) and platy kaolinite (Kaol) used in this study were collected from Linfen, Shanxi Province, China, and Maoming, Guangdong Province, China, respectively. The physical sedimentation method (Du et al., 2018) was used to purify the tubular halloysite. The chemical compositions (mass %) of the samples measured by X-ray fluorescence spectroscopy were shown in Table 1. Both the samples were sieved through a 200-mesh sieve.

2.2. Sorption experiments

All sorption experiments were conducted in 50-mL polypropylene copolymer centrifuge tubes. For each experiment, the sample (30.0 mg) and Eu(III) solution (20.0 mL) with 0.01 mol/L $NaNO_3$ as background electrolyte (Yang et al., 2019) were mixed in the centrifuge tubes, which was then placed on a shaker (200 rpm and 25°C) for 24 h. The initial concentration of Eu(III) was from 0.03 to 9.16 mg/L. The initial pH in the batch sorption experiments was 4.0, 5.0, or 6.0, similar to that in WED-RE ores (Bao and Zhao, 2008), which was adjusted using NaOH and/or HNO_3 solution. The Eu(III) ions used in the batch sorption experiments were obtained by dissolving Eu_2O_3 (99.9%) in HNO_3

Table 1
Chemical compositions of Hal and Kaol (%).

Sample	Al_2O_3	SiO_2	CaO	Fe_2O_3	MgO	K_2O	Na_2O	TiO_2	IL (loss on ignition)
Hal	37.64	43.72	0.44	0.31	0.08	0.10	0.11	0.22	16.89
Kaol	36.48	47.69	0.08	0.69	0.11	0.65	0.07	0.36	13.47

(Bradbury and Baeyens, 2002). Then supernatant and solid clay minerals (Hal/Eu and Kaol/Eu) were collected for further analysis by centrifugation at 11000 rpm for 5 min.

Similarly, for the sorption kinetics experiments, the sample (30 mg) and Eu(III) solution (20 mL) were mixed in 50-mL centrifuge tubes, which were then placed on a shaker (200 rpm and 25°C) for 0.08, 0.33, 0.67, 1, 2, 12, or 24 h. The initial pH value was 5 and the initial Eu(III) concentration was 4.90×10^{-5} mol/L. All supernatants were collected by centrifuging at 11000 rpm for 2 min. Ultra-pure water (18.25 MΩ/cm) was used throughout the experiments and all reagents were purchased from Shanghai Aladdin Biochemical Technology Co. Ltd.

2.3. Desorption experiments

Desorption experiments were conducted using Hal and Kaol pre-adsorbed with Eu(III) (hereinafter denoted Hal-Eu and Kaol-Eu, respectively), which were prepared by mixing the corresponding sample (3 g) and $Eu(NO_3)_3$ solution (30 mL) into 50-mL centrifuge tubes at pH 5. The concentration of the $Eu(NO_3)_3$ solution was 2.63×10^{-3} for Hal and 1.34×10^{-3} mol/L for Kaol. The suspensions were shaken at 200 rpm for 24 h then centrifuged at 11000 rpm for 5 min to obtain Hal-Eu and Kaol-Eu. The separated samples were dried in an oven at 60°C then sieved through a 200-mesh sieve prior to use in the desorption experiments.

Batch desorption of Eu(III) from Hal-Eu or Kaol-Eu was studied using $(NH_4)_2SO_4$ solution, which is one of the most common extractants (Moldoveanu and Papangelakis, 2013). The sample (100 mg) samples and $(NH_4)_2SO_4$ solution (30 mL) were mixed in 50-mL centrifuge tubes and placed on a shaker (200 rpm and 25°C) for 24 h. The concentrations of the $(NH_4)_2SO_4$ solution were 0.001, 0.01, and 0.1 mol/L. The desorption efficiency of REE(III) increases with the increasing concentration $(NH_4)_2SO_4$, it is not sensitive to $(NH_4)_2SO_4$ concentration in the range 0.1–2.5 mol/L (Moldoveanu and Papangelakis, 2013). About 98.5% exchangeable REE(III) ions were extracted by ~0.15 mol/L $(NH_4)_2SO_4$ with the solid/liquid ratio of 1 g/mL (Li, 2014), which indicates almost exchangeable Eu(III) ions on Hal-Eu and Kaol-Eu were desorbed when $(NH_4)_2SO_4$ concentration is 0.1 mol/L. The supernatants for the subsequent analysis were collected by centrifuging the reaction suspensions at 11000 rpm for 5 min.

Column desorption experiments were conducted using a quartz tube with a diameter of 2 cm (Fig. 1). The pre-adsorbed samples (1.00 g) and quartz sand (2.00 g) were mixed homogeneously to increase the hydraulic conductivity and avoid blocking the flow of the $(NH_4)_2SO_4$ solution. This mixture was then packed into the column and 0.001 mol/L $(NH_4)_2SO_4$ solution was pumped upward through the column continuously at a rate of 1 mL/min, which was controlled by a peristaltic pump. For the first 30 min, the eluate at the column outlet was collected into 15-mL centrifuge tubes continuously with a collection time of 3 min per fraction. At the end of this period, one sample of the eluate was collected every 10 min with a collection time of 3 min per fraction in the middle of the 10 min.

2.4. Characterization methods

X-ray diffraction (XRD) patterns of halloysite and kaolinite were recorded on a Bruker D8 Advance diffractometer (Mannheim, Germany) with a Ni filter and Cu Kα radiation (λ = 0.154 nm) generated at 40 kV and 40 mA (Du et al., 2018). The XRD patterns were measured from 3° to 70° (2θ) at a scanning rate of 3°/min.

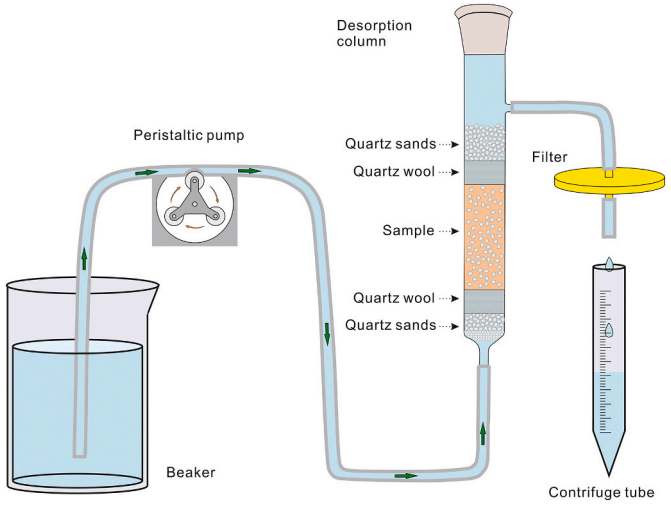

Fig. 1. Diagram of the column desorption experiment.

The SSA of the samples was measured using a Micromeritics ASAP2020 system at liquid-nitrogen temperature and calculated using the multiple-point Brunauer-Emmett-Teller (BET) method. The samples were outgassed at 120°C for 12 h prior to the measurements.

Scanning electron microscopy (SEM) images of halloysite and kaolinite were obtained using a JEOL JSM 7610F field-emission scanning electron microscope. Transmission electron microscopy (TEM) images were recorded on an FEI Talos F200S field-emission transmission electron microscope operating at an accelerating voltage of 200 kV. Halloysite and kaolinite were ultrasonically dispersed in ethanol for 6 min, and then two droplets were loaded onto a carbon-coated copper grid to prepare the specimens for TEM measurement.

The Eu(III) concentration was measured by ICP-MS on a Thermo-Scientific iCAP Qc with a precision of better than 5%. The Hal/Eu and Kaol/Eu samples obtained from the sorption experiments at pH 5 were characterized using a Thermo Fisher Scientific (UK) K-Alpha X-ray photoelectron spectrometer with a monochromatic Al Kα X-ray source (excitation energy = 1468.6 eV). The XPS analysis chamber was evacuated to ultra-high vacuum (the pressure of 5×10^{-8} mbar or lower) prior to the analysis. Spectra were collected from 0 to 1350 eV using an X-ray spot size of 400 μm with a pass energy of 100 eV for wide scan and 30 eV for individual elements. The binding energies were corrected relative to the carbon 1 s signal at 284.8 eV (; Liu et al., 2016b). The adsorbed amounts (mass%) of Eu on the Hal/Eu and Kaol/Eu samples detected by XPS were calculated using the following equation:

$$Q = \frac{N_{Eu} \times M_{Eu}}{\sum N_i \times M_i}$$

where Q is the adsorbed amount (mass %) of Eu, i denotes an element detected by XPS (e.g., Eu, Si, Al, and O), and N and M are the atomic content of the corresponding element and its atomic mass, respectively.

3. Results and discussion

3.1. Structural characteristics of Hal and Kaol

The XRD patterns of Hal and Kaol revealed that both samples

possessed high purity and crystallinity (Fig. 2a). The peak at approximately 11.7° with a *d*-value of 0.74 nm in the XRD pattern was assigned to the typical (001) reflection of the halloysite (7 Å). The broad reflection at approximately 0.72–0.76 nm is attributable to the tubular morphology (Fig. 2b and c), small crystal size, and a high degree of disorder (Joussein et al., 2005). As shown in the TEM images, the length of the tubes ranged from approximately 0.2–2.0 μm, while the external and internal diameters were approximately 30–70 nm and 10–30 nm, respectively. The d_{001}-value of Kaol (Fig. 2c) is was approximately 0.72 nm (Fig. 2a). The diameter of Kaol ranged from sub-micrometers to several micrometers (Fig. 2d and e), which is in good agreement with that reported kaolinite in weathered crusts (Zhou et al., 2018). The SSA of Hal (68.14 m^2/g) was almost five times larger than that of Kaol (13.89 m^2/g).

3.2. Sorption of Eu(III) on Hal and Kaol and their mechanisms

The sorption characteristics of Eu(III) on Hal and Kaol were investigated at various pH values of 4.0, 5.0, and 6.0. Fig. 3 exhibits the sorption isotherms fitted by the well-known Freundlich and Langmuir models (Goldberg et al., 2007). The higher correlation coefficient (R^2, >0.9) for the Freundlich model suggests that the sorption isotherms were better fitted by this model than by the Langmuir model. These results imply the sorption of Eu(III) ions on the heterogeneous surfaces of Hal and Kaol (Ng et al., 2002). The sorption amount of Eu(III) was higher for Hal than for Kaol (Figs. 3 and 4). In addition, the pH exerted a significant influence on the sorption behavior of Eu(III) on Hal (Fig. 3), with the sorption amount increasing by 53.55% from 3.38 to 5.19 mg/g. In contrast, the sorption amount for Kaol increased by only 13.76% from 1.89 to 2.15 mg/g. The increase in the sorption amounts with increasing pH was ascribed to the deprotonation of hydroxyl groups on the surfaces of the minerals (Bradbury and Baeyens, 2002; Coppin et al., 2002), implying the interaction between Eu(III) ions and hydroxyl groups.

Fig. 4 shows the Eu(III) sorption kinetics on Hal and Kaol, which were well-fitted by pseudo-second-order kinetic models, with R^2 values of 0.99995 and 1, respectively. The sorption amounts at equilibrium for Hal and Kaol were 4.2 and 1.6 mg/g, while the sorption efficiencies were approximately 84% and 32%, respectively (Fig. 4b). These results demonstrate the difference in sorption capacity between the two minerals. The sorption reactions reached equilibrium within 20 min and the rate of Eu(III) sorption was faster for Hal than for Kaol (Fig. 4b).

The XPS spectra of these samples were recorded after sorption to examine the chemical state of the Eu on Hal and Kaol. Fig. 5 displays the Eu $3d_{5/2}$ spectra obtained for Hal/Eu and Kaol/Eu, which demonstrated that the Eu(III) ions had been adsorbed onto both samples. According to the XPS results, the elemental contents (atom %) were as follow: Hal/Eu, 14.83% Al, 18.21% Si, 66.91% O, and 0.05% Eu; Kaol/Eu, 14.89% Al, 18.03% Si, 67.06% O, and 0.02% Eu. Thus, the adsorbed amounts (mass %) of Eu on Hal/Eu and Kaol/Eu were calculated to be approximately 0.38% and 0.15% respectively, which were similar to the results of the sorption experiment (Fig. 3).

Table 2 lists the multiplet peak parameters of Eu $3d_{5/2}$ on Hal/Eu and Kaol/Eu. In the Eu $3d_{5/2}$ spectrum of Hal/Eu, two peaks were observed at different binding energies (Fig. 5a). The presence of multiple peaks at different binding energies generally indicates different chemical states of Eu, such as $Eu(NO_3)_3$ (1136.4 eV) and $Eu_2(CO_3)_3$ (1135.5 eV) (Mercier et al., 2006). The binding energies of Eu $3d_{5/2}$ photoelectron peaks from some different chemical species were summarized in Table S1. Thus, the peaks at 1134.46 and 1137.40 eV for Hal/Eu suggested the presence of two distinct chemical species. The former was attributed to the inner-sphere complexes of Eu (Kowal-Fouchard et al., 2004; Fan et al., 2009), originating from the reaction between the aluminum hydroxyl groups of halloysite and Eu(III) ions (Bradbury and Baeyens, 2002, 2009; Wang et al., 2015); while the latter was ascribed to the outer-sphere complexes of Eu (Kowal-Fouchard et al., 2004). Similarly, the peaks at 1134.48 and 1137.69 eV in the Eu $3d_{5/2}$ spectrum of Kaol/Eu (Fig. 5b) were assigned to the inner-sphere complexes and outer-sphere complexes, respectively. Therefore, the main Eu(III) sorption mechanisms on Hal and Kaol were inner-sphere complexation and outer-sphere complexation.

The species of Eu(III) in solution is dominated by Eu^{3+} ions coordinated with 8 or 9 water molecules in weakly acidic environments with pH values ranging from 4 to 6 (Bau, 1999; Diaz-Moreno et al., 2000; Tanaka et al., 2008; Bradbury and Baeyens, 2002; Borst et al., 2020). Both halloysite and kaolinite have numerous hydroxyl groups on their surface, e.g., the aluminol surface (Yuan et al., 2008). Moreover, the two minerals possess permanent negative charges resulting from isomorphous substitution (e.g., Al^{3+} replaces Si^{4+} in the tetrahedral sheet)

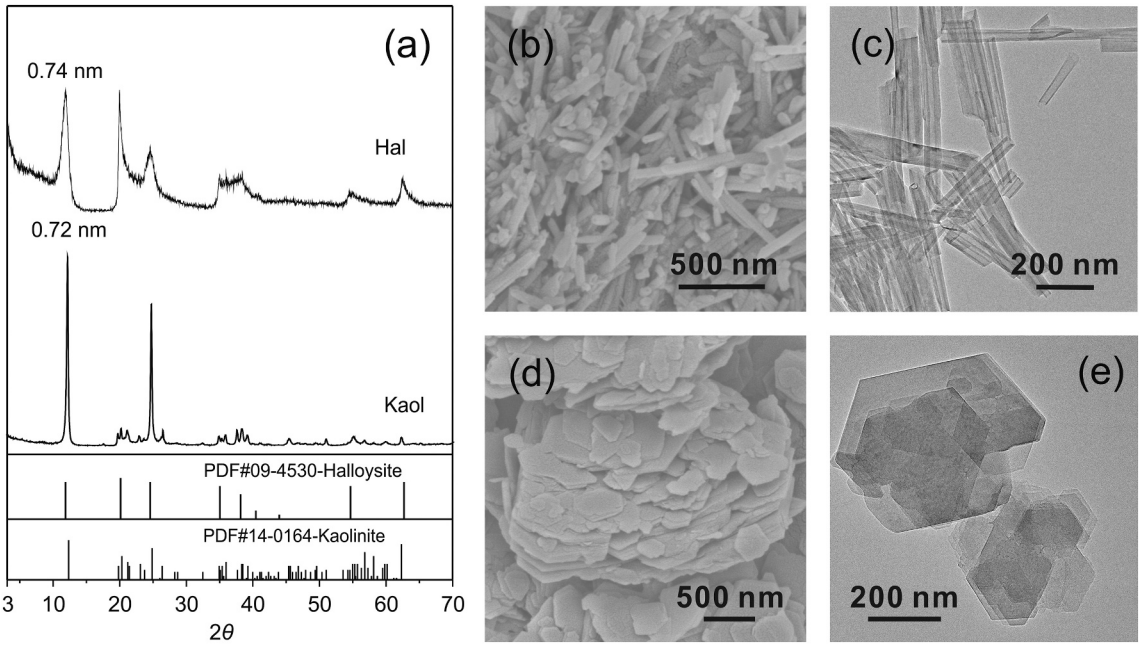

Fig. 2. XRD patterns of Hal and Kaol (a); SEM (b) and TEM (c) images of Hal; SEM (d) and TEM (e) images of Kaol.

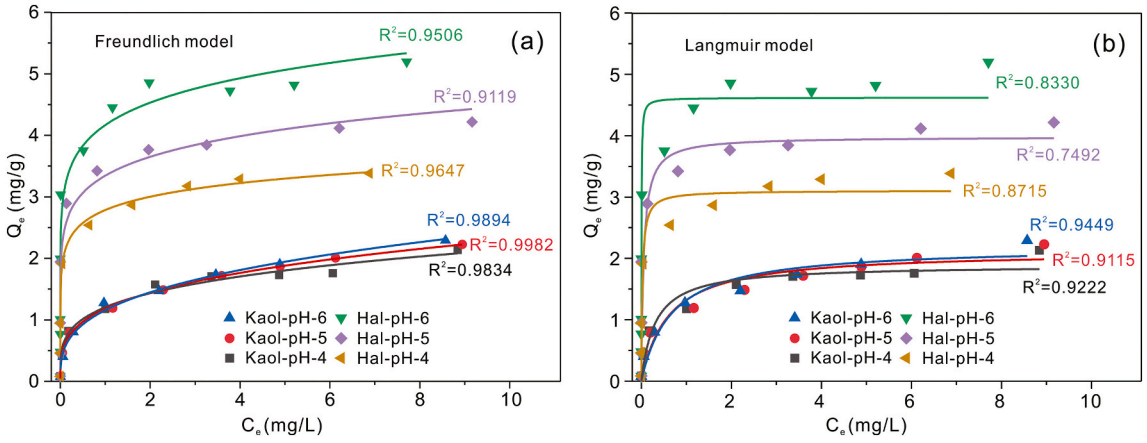

Fig. 3. Eu(III) sorption isotherms fitted by Freundlich (a) and Langmuir (b) models under different pH values (4.0, 5.0, and 6.0), I = 0.01 mol/L $NaNO_3$, S:L = 1.5 g/L.

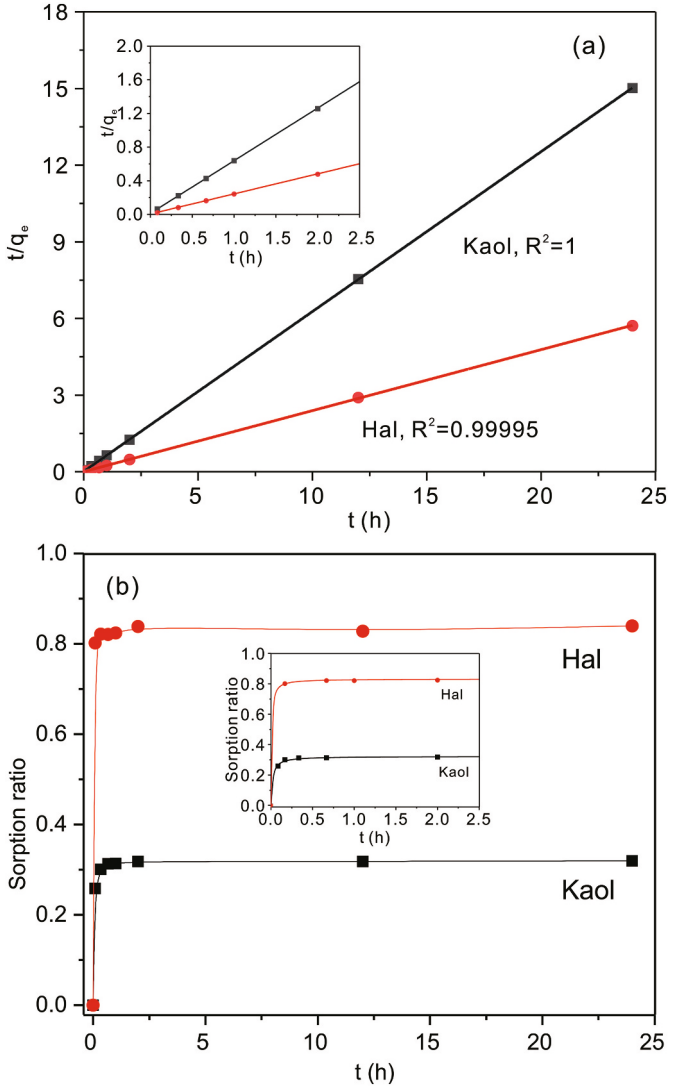

Fig. 4. (a) Sorption kinetics of Eu(III) onto Hal and Kaol fitted by pseudo-second-order model and the inset is the magnification of the sorption kinetics at time 0–2.5 h. (b) Sorption ratio of Eu(III) onto halloysite and kaolinite with increasing time and the inset is the magnification of the sorption ratio at time 0–2.5 h. pH = 5, I = 0.01 mol/L $NaNO_3$, S:L = 1.5 g/L.

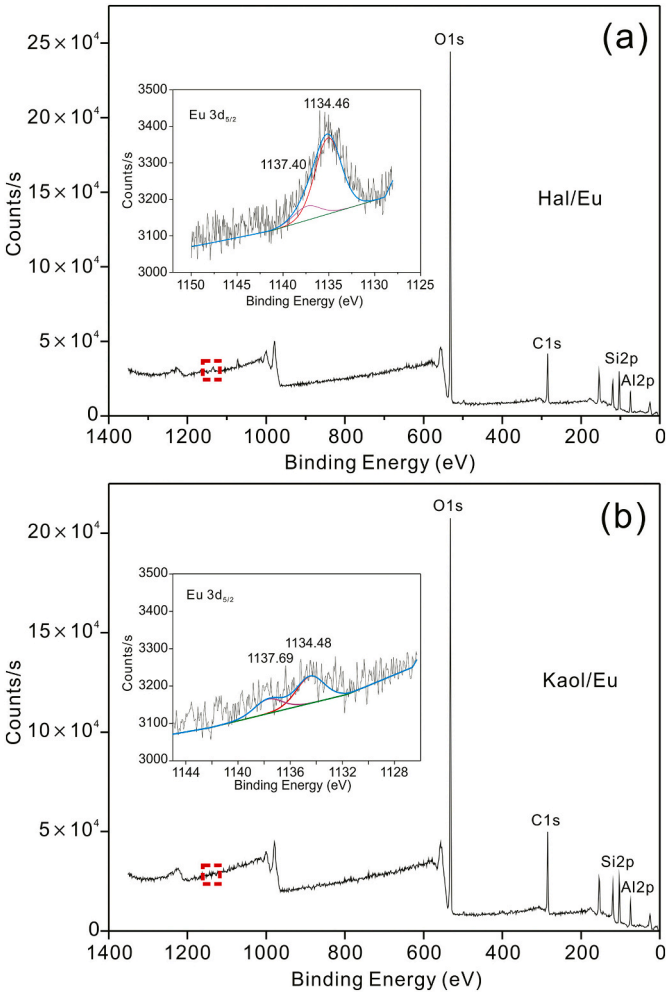

Fig. 5. Survey spectrum of Hal/Eu (a) and Kaol/Eu (b) in the pH value of 5; the insets show their Eu $3d_{5/2}$ spectra.

(Joussein et al., 2005) and variable charges due to surface breakage and defects (Bergaya et al., 2013). Thus, the sorption processes were the interaction between the Eu^{3+} ions and the surfaces of halloysite and kaolinite.

The content ratios between the inner-sphere complexes and outer-sphere complexes for Kaol/Eu and Hal/Eu are approximately 3:2 and

Table 2
Eu $3d_{5/2}$ binding energy (eV) and area ratio of the Eu(III) Hal/Eu and Kaol/Eu.

Sample	Atomic content (%)	Binding energy (eV)	Area ratio between former and latter peaks
Hal/Eu	0.05	1134.46, 1137.40	~ 3:1
Kaol/Eu	0.02	1134.48, 1137.69	~ 3:2

~ 3:1, respectively, based on the area ratios of the two corresponding peaks (Table 2). These data implied that the inner-sphere complexation between the aluminum hydroxyl groups and Eu^{3+} ions was the primary mechanism of Eu(III) sorption on both Hal and Kaol. The differences in the influence of pH on the sorption (Fig. 3) by the two minerals and in their sorption capacity primarily resulted from the inner-sphere complexation due to their different microstructures and surface properties, such as the larger SSA and more OH groups of halloysite than kaolinite (Yang et al., 2019). Kaolinite possesses a platy morphology with a considerable number of aluminum hydroxyl groups at the edges and surface defects of the particles, whereas halloysite has a distinct nano-sized tubular morphology and its internal surface contains numerous aluminum hydroxyl groups (Yuan et al., 2008), in addition to the hydroxyl groups at the edges and surface defects of particles. Moreover, outer-sphere complexation accounted for approximately 40% and 25% of the Eu(III) adsorbed on Kaol and Hal, respectively (Table 2). Thus, although the sorption amounts by outer-sphere complexation were lower than those by inner-sphere complexation, outer-sphere complexation still plays an important role in the Eu(III) sorption by these minerals.

As mentioned above, REE have similar geochemical properties, and commonly migrate and accumulate together as a group (Henderson, 1984). Similar to Eu, all of the REE species in a weak acidic solution predominantly exist as hydrated REE^{3+} ions (Bau, 1999). Therefore, halloysite has a higher sorption capacity for REE(III) ions than kaolinite and the inner-sphere complexation is the primary sorption mechanism. However, Borst et al. (2020) thought the occurrence of REE(III) in WED-RE ores was outer-sphere complexes according to the results of synchrotron X-ray absorption spectroscopy, which is different from the results of sorption experiments. This discrepancy might be due to the difference in sorption conditions between weathered crusts and pure clay minerals. For example, the Eu(III) concentration in the sorption experiment is far higher than the REE(III) concentration in the rainwater or groundwater. Meanwhile, the pH in the deeper horizon of weathered profiles commonly is higher than that in the upper horizon, which indicates the clay minerals in the deeper horizon could have a higher capacity for REE(III) sorption, according to sorption results.

3.3. Eu(III) desorption from clay and its implications

Besides sorption, desorption is another important process governing REE(III) migration and enrichment in weathered crusts. Fig. 6a shows the batch desorption results of Eu(III) from Hal-Eu and Kaol-Eu under various extractant concentrations. After exposure into $(NH_4)_2SO_4$ solution at concentrations of 0.001, 0.01, and 0.1 mol/L for 24 h, the desorption amounts of Eu(III) were 0.10, 2.12, and 2.63 mg/g for Hal-Eu respectively and 0.19, 0.88, and 0.94 mg/g for Kaol-Eu, respectively (Fig. 6a). Thus, the desorption efficiency increased with the increasing concentration of NH_4^+ ions. There are still some active sites on Hal-Eu and Kaol-Eu. In the suspension, NH_4^+ ions with low $-\Delta H_{hydation}$ (322 kJ/mol) (Moldoveanu and Papangelakis, 2012) could be adsorbed onto the surfaces of the clay minerals to form strong electrostatic bonds, whereas Eu(III) ions with high $-\Delta H_{hydation}$ (3508 kJ/mol) form comparatively weak bonds on the surfaces (Miller et al., 1982; Moldoveanu and Papangelakis, 2012). Therefore, the Eu(III) ions are easily displaced from the clay minerals by the NH_4^+ ions at a 3:1 NH_4^+:Eu(III) stoichiometry (Moldoveanu and Papangelakis, 2012).

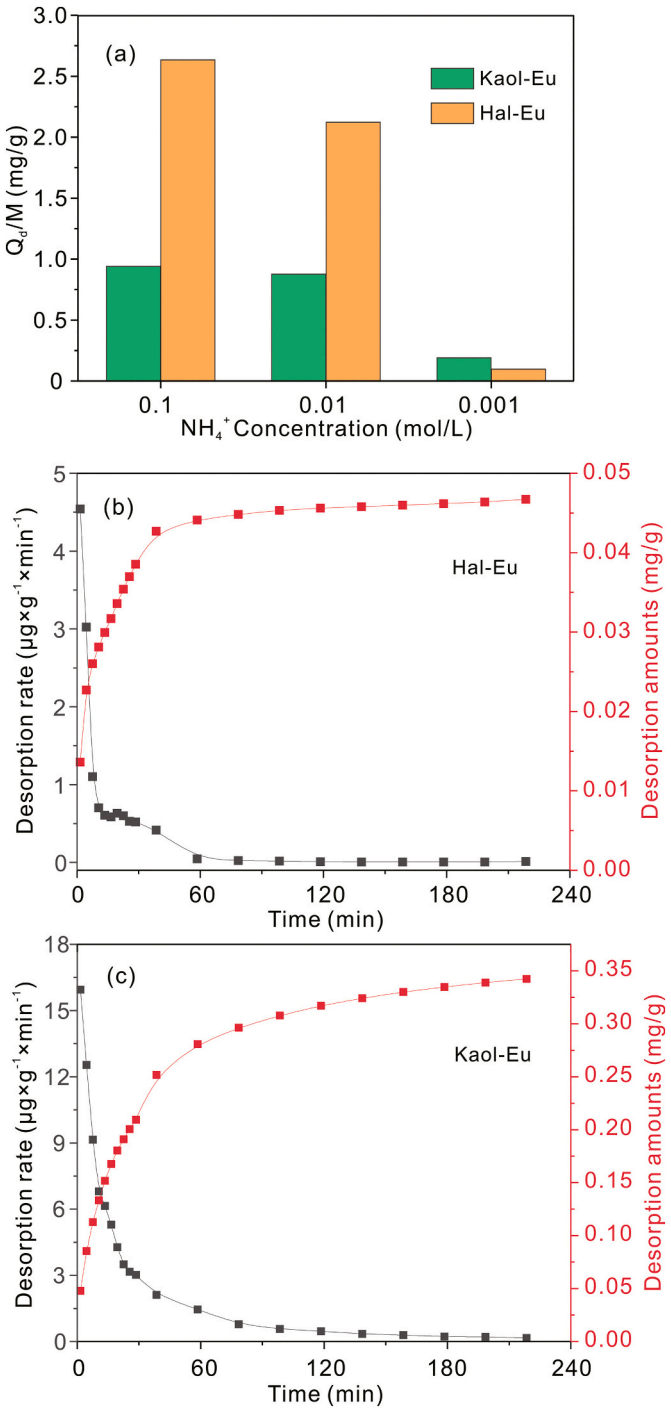

Fig. 6. (a) Amount of Eu(III) desorption under the NH_4^+ concentration of 0.2, 0.02, and 0.002 mol/L in batch desorption. The desorption rate and total amounts of desorption from Hal-Eu (b) and Kaol-Eu (c) with increasing time in column desorption.

Compared to batch desorption, column desorption is more realistic for simulating the conditions of weathered crusts (Allen et al., 1995), and the results are shown in Fig. 6b and c. In the case of Hal-Eu, the desorption rate decreased from approximately 4.54 to 5.00 × 10^{-3} μg/(g·min) with increasing time (Fig. 6b). The rate decreased rapidly during the first stage of the experiment (0–40 min) and then more slowly during the second stage (40–220 min). The final desorption amount of Eu(III) was approximately 0.05 mg/g, ~91% of which occurred during the first

stage (Fig. 6b), suggesting that the desorption of Eu(III) from Hal-Eu primarily took place within the first 40 min.

Similarly, the Eu(III) desorption rate also decreased with increasing time for Kaol-Eu, changing from 15.94 to 0.17 μg/(g·min) (Fig. 6c), which was higher than that observed for Hal-Eu. The desorption rate also decreased rapidly during the first stage of the experiment (0–40 min) and more slowly during the second stage (40–220 min). The final desorption amount (0.34 mg/g) for Kaol-Eu was higher than that for Hal-Eu, in accordance with the batch desorption results (Fig. 6a). Nevertheless, only 74% of the desorption occurred during the first stage, indicating that Hal-Eu reached its desorption equilibrium more rapidly than Kaol-Eu (Fig. 6c).

The desorption is an exchange reaction between the Eu(III) ions on the surfaces of the clay minerals and the NH_4^+ ions in the extraction solution, which is influenced by the reactant concentration, temperature, and nature of the reactant (Connors, 1990). In general, a high reactant concentration should facilitate the desorption reaction and lead to a high amount of desorption (Connors, 1990), such as the higher desorption amounts of Eu(III) from Hal-Eu than that from Kaol-Eu as the NH_4^+ concentration was 0.2 or 0.02 mol/L (Fig. 6a). But the Kaol-Eu displayed a higher amounts of Eu(III) desorption than Hal-Eu when NH_4^+ concentration was 0.002 mol/L (Fig. 6a). According to the sorption characteristics, the exchangeable Eu(III) on Hal-Eu and Kaol-Eu did not reach their highest sorption amounts, which indicates they still could have some active sites to adsorb NH_4^+. Consequently, the NH_4^+ concentration would decrease in extracting solution, giving rise to the inverse desorption phenomenon when NH_4^+ concentration was 0.002 mol/L.

In addition, this reaction should be closely associated with the interaction force between the clay minerals and Eu(III) ions. As demonstrated by the sorption results, Eu(III) adsorbed on the halloysite and kaolinite were inner-sphere complexes and outer-sphere complexes. The outer-sphere complexes generally have a weaker affinity with clay minerals than inner-sphere complexes (Goldberg, 2013), which suggests the desorption of outer-sphere complexes should occur first. The desorption amounts (Fig. 6) imply that the desorbed Eu(III) ions are dominating outer-sphere complexes at the NH_4^+ solution of 0.002 mol/L. Although Hal-Eu has more exchangeable Eu(III) ions than Kaol-Eu, the desorption rate of Eu(III) from Hal-Eu was much lower than that from Kaol-Eu in the column desorption experiment (Fig. 6b), which could be related to the steric effect of halloysite tubes. Compared to the batch desorption experiment, column desorption provided enough NH_4^+ ions to exchange the Eu(III) ions. But the final desorption amount of Eu (III) from Hal-Eu was still lower than that from Kaol-Eu (Fig. 6b and c), which indicates the difference in electrostatic attraction between Eu(III) and two clay minerals. Although halloysite and kaolinite possess the similar chemical composition and are both composed of octahedral sheet and tetrahedral sheet (Joussein et al., 2005; Yuan et al., 2015), the former has a tubular morphology due to the misfit of the two sheets, which give rise to some differences in the crystal structure (e.g., lattice parameters) between the two minerals (Singh, 1996; Detellier and Schoonheydt, 2014). These differences may gives rise to the slightly stronger attraction between tubular halloysite and outer-sphere complexes of Eu(III) than that for platy kaolinite, resulting in a higher rate and amount of desorption from Kaol-Eu than Hal-Eu (Fig. 6).

As mentioned above, REE have similar geochemical properties during geological processes and typically migrate and accumulate together as a group (Henderson, 1984). Similar to Eu, all of the REE species in a weak acidic solution predominantly exist as REE(III) ions (Bau, 1999). Moreover, in weathered crusts, the mean concentration of cations (e.g., Na^+, Mg^{2+}, NH_4^+, K^+, and Ca^{2+}) is generally 0.002–0.004 mol/L in rainwater/groundwater (Edmeades et al., 1985; Huang et al., 2013; Zhang et al., 2015), which is similar to the NH_4^+ concentration in the column desorption experiments. These cations have low $-\Delta H_{hydation}$ (e.g., 406 kJ/mol for Na^+) and can also establish strong electrostatic bonds like the NH_4^+ ion (Miller et al., 1982; Moldoveanu and Papangelakis, 2012). Thus, as implied by the desorption results (Fig. 6b and c), the tubular halloysite could have a lower rate and amount of REE(III) desorption than platy kaolinite in weathered crusts. This means, very likely, that the tubular halloysite has a stronger retention capacity (Fig. 6) for exchangeable REE(III) ions than platy kaolinite in the weathered crusts. Furthermore, the tubular halloysite has a higher adsorption capacity (Fig. 4). In addition, the occurrence of hydrated halloysite (i.e., halloysite (10 Å)) in weathered crusts could also lead to the increasing sorption of REE ions (Ram et al., 2019). Moreover, a greater REE recovery has been reported when halloysite is present in the weathered crusts (Burcher-Jones et al., 2018). In this sense, the halloysite may play a more important role in REE enrichment than kaolinite in WED-RE ores and deserves more research attention in the future. Notably, the contribution of halloysite and kaolinite on REE(III) accumulation in WED-RE ores depends on their content, although halloysite has a higher capacity for enriching REE(III) ions than kaolinite.

4. Conclusions

In this study, the sorption and desorption of Eu(III) on halloysite and kaolinite were investigated to elucidate the geochemical behaviors (accumulation and migration) of REE(III) ions in WED-RE ores. The obtained results reveal that the tubular halloysite has a higher sorption capacity for Eu(III) ions than kaolinite. The amounts of Eu(III) adsorbed onto the halloysite and kaolinite increased as the pH increased from 4.0 to 6.0. Two Eu species were adsorbed on the surface of both minerals through inner-sphere complexation and outer-sphere complexation. Inner-sphere complexation between aluminum hydroxyl groups and Eu (III) ions is the primary mechanism of Eu sorption on both clay minerals.

The Eu(III) ions were easily desorbed by exchange with NH_4^+ ions and the desorption amount increased with increasing $(NH_4)_2SO_4$ concentration. Halloysite displayed higher desorption amounts of Eu(III) than kaolinite when NH_4^+ concentrations were 0.2 or 0.02 mol/L, but lower desorption amount when the NH_4^+ concentration was 0.002 mol/L. The desorption rate of Eu(III) from kaolinite was higher than that from the halloysite at NH_4^+ concentration of 0.002 mol/L. Moreover, the desorption occurred more easily from kaolinite than halloysite, which was likely determined by the attraction between the outer-sphere complexes and the clay minerals.

The tubular halloysite has a higher sorption capacity and stronger retention capacity for Eu(III) than platy kaolinite in the environment of weathered crusts, indicating that halloysite could be more favorable for Eu(III) enrichment than kaolinite. Considering the expected similar sorption and desorption characteristics of REE(III) ions, the tubular halloysite may make a larger contribution to the sorption and retention for REE than platy kaolinite in WED-RE ores. These fundamental results provide novel insights into the enrichment and migration of REE and the role of clay minerals in REE enrichment during ore formation.

CRediT author statement

All persons who meet authorship criteria are listed as authors, and all authors certify that they have participated sufficiently in the work. **Junming Zhou:** Conceptualization, Investigation, Resources, Data Curation, Writing – Original Draft, Visualization. **Hongmei Liu**: Investigation. **Dong Liu**: Conceptualization, Writing – Review & Editing, Supervision. **Peng Yuan**: Conceptualization, Writing – Review & Editing, Supervision, Funding acquisition. **Hongling Bu**: Investigation, Funding acquisition. **Peixin Du**: Investigation, Resources. **Wenxiao Fan**: Review & Editing. **Mengyuan Li**: Investigation.

Declaration of Competing Interest

The authors declare that they have no known competing financial interests or personal relationships that could have appeared to influence the work reported in this paper.

Acknowledgments

This work was financially supported by the National Special Support for High-Level Personnel, National Natural Science Foundation of China (Grant No. 41972045), GDAS' Project of Science and Technology Development (Grant No. 2020GDASYL-20200102019), and Science and Technology Planning of Guangdong Province, China (Grant No. 2020B1212060055). This is a contribution No.IS-3100 from GIGCAS.

Appendix A. Supplementary data

Supplementary data to this article can be found online at https://doi.org/10.1016/j.clay.2021.106356.

References

Allen, H.E., Chen, Y.T., Li, Y.M., Huang, C.P., Sanders, P.F., 1995. Soil partition-coefficients for Cd by column desorption and comparison to batch adsorption measurements. Environ. Sci. Technol. 29, 1887–1891.
Aparicio, P., Galán, E., Valdrè, G., Moro, D., 2009. Effect of pressure on kaolinite nanomorphology under wet and dry conditions. Correlation with other kaolinite properties. Appl. Clay Sci. 46, 202–208.
Banfield, J.F., Eggleton, R.A., 1990. Analytical transmission electron microscopy studies of plagioclase, muscovite, and K-feldspar weathering. Clay Clay Miner. 38 (1), 77–89.
Bao, Z.W., Zhao, Z.H., 2008. Geochemistry of mineralization with exchangeable REY in the weathering crusts of granitic rocks in South China. Ore Geol. Rev. 33, 519–535.
Bau, M., 1999. Scavenging of dissolved yttrium and rare earths by precipitating iron oxyhydroxide: experimental evidence for Ce oxidation, Y-Ho fractionation, and lanthanide tetrad effect. Geochim. Cosmochim. Acta 63 (1), 67–77.
Bergaya, F., Theng, B.K.G., Lagaly, G., 2013. Handbook of Clay Science, Second edition. Elsevier.
Borst, A.M., Smith, M.P., Finch, A.A., Estrade, G., Villanova-de-Benavent, C., Nason, P., Marquis, E., Horsburgh, N.J., Goodenough, K.M., Xu, C., Kynicky, J., Geraki, K., 2020. Adsorption of rare earth elements in regolith-hosted clay deposits. Nature. Communications 11.
Bradbury, M.H., Baeyens, B., 2002. Sorption of Eu on Na- and Ca-montmorillonites: experimental investigations and modelling with cation exchange and surface. Geochim. Cosmochim. Acta 66, 2325–2334.
Bradbury, M.H., Baeyens, B., 2009. Sorption modelling on illite Part I: titration measurements and the sorption of Ni, Co, Eu and Sn. Geochim. Cosmochim. Acta 73 (4), 990–1003.
Burcher-Jones, C., Mkhize, S., Becker, M., Ram, R., Petersen, J., 2018. Study of the deportment of REEs in ion adsorption clays towards the development of an in situ leaching strategy. In: Extraction 2018. Springer, Cham, pp. 2429–2439.
Chakhmouradian, A.R., Wall, F., 2012. Rare earth elements: minerals, mines, magnets (and more). Elements 8, 333–340.
Chen, Z., Zhang, Z., Chi, R., 2020. Leaching process of weathered crust elution-deposited rare earth ore with formate salts. Front. Chem. 8.
Chi, R.A., Tian, J., 2008. Weathered Crust Elution-Deposited Rare Earth Ores. Nova Science Publishers, New York.
Connors, K.A., 1990. Chemical Kinetic: The Study of Reaction Rate in Solution. VCH publishers, Inc.
Coppin, F., Berger, G., Bauer, A., Castet, S., Loubet, M., 2002. Sorption of lanthanides on smectite and kaolinite. Chem. Geol. 182, 57–68.
Detellier, C., Schoonheydt, R.A., 2014. From platy kaolinite to nanorolls. Elements 10, 201–206.
Diaz-Moreno, S., Munoz-Paez, A., Chaboy, J., 2000. X-ray absorption spectroscopy (XAS) study of the hydration structure of yttrium(III) cations in liquid and glassy states: eight or nine-fold coordination? J. Phys. Chem. A 104, 1278–1286.
Du, P., Liu, D., Yuan, P., Deng, L., Wang, S., Zhou, J., Zhong, X., 2018. Controlling the macroscopic liquid-like behaviour of halloysite-based solvent-free nanofluids via a facile core pretreatment. Appl. Clay Sci. 156, 126–133.
Dutta, T., Kim, K.H., Uchimiya, M., Kwon, E.E., Jeon, B.H., Deep, A., Yun, S.T., 2016. Global demand for rare earth resources and strategies for green mining. Environ. Res. 150, 182–190.
Edmeades, D.C., Wheeler, D.M., Clinton, O.E., 1985. The chemical-composition and ionic-strength of soil solution from New-Zealand topsoils. Aust. J. Soil Res. 23, 151–165.
Estrade, G., Marquis, E., Smith, M., Goodenough, K., Nason, P., 2019. REE concentration processes in ion adsorption deposits: evidence from the Ambohimirahavavy alkaline complex in Madagascar. Ore Geol. Rev. 112, 103027.
Fan, Q.H., Tan, X.L., Li, J.X., Wang, X.K., Wu, W.S., Montavon, G., 2009. Sorption of Eu (III) on attapulgite studied by batch, XPS, and EXAFS techniques. Environ. Sci. Technol. 43, 5776–5782.
Goldberg, S., 2013. Surface Complexation Modeling. Ref. Module Earth Syst. Environ. Sci. https://doi.org/10.1016/B978-0-12-409548-9.05311-2.
Goldberg, S., Criscenti, L.J., Turner, D.R., Davis, J.A., Cantrell, K.J., 2007. Adsorption – desorption processes in subsurface reactive transport modeling. Vadose Zone J. 6, 407–435.
Henderson, P., 1984. General geochemical properties and abundances of the rare earth elements. In: Henderson, P. (Ed.), Rare Earth Element Geochemistry. Elsevier, New York.
Huang, G.X., Sun, J.C., Zhang, Y., Chen, Z.Y., Liu, F., 2013. Impact of anthropogenic and natural processes on the evolution of groundwater chemistry in a rapidly urbanized coastal area, South China. Sci. Total Environ. 463, 209–221.
Joussein, E., Petit, S., Churchman, J., Theng, B., Righi, D., Delvaux, B., 2005. Halloysite clay minerals - a review. Clay Min. 40, 383–426.
Keller, W.D., 1978. Classification of kaolins exemplified by their textures in scan electron micrographs. Clay Clay Miner. 26, 1–20.
Kowal-Fouchard, A., Drot, R., Simoni, E., Marmier, N., Fromage, F., Ehrhardt, J.J., 2004. Structural identification of europium(III) adsorption complexes on montmorillonite. New J. Chem. 28 (7), 864–869.
Kynicky, J., Smith, M.P., Xu, C., 2012. Diversity of rare earth deposits: the key example of China. Elements 8 (5), 361–367.
Li, Y.X., 2014. Ion Adsorption Rare Earth Resources and Their Green Extraction. Chemical Industry Press, pp. 159–207.
Li, Y.H.M., Zhao, W.W., Zhou, M.F., 2017. Nature of parent rocks, mineralization styles and ore genesis of regolithhosted REE deposits in South China: an integrated genetic model. J. Asian Earth Sci. 148, 65–95.
Li, M.Y.H., Zhou, M.F., Williams-Jones, A.E., 2019. The genesis of regolith-hosted heavy rare earth element deposits: insights from the world-class Zudong deposit in Jiangxi province, South China. Econ. Geol. 114, 541–568.
Liu, R., Wang, R.C., Lu, X., Li, J., 2016a. Nano-sized rare earth minerals from granite – related weathering – type REE deposits in southern Jiangxi. Acta Petrol. Mineral. 35 (4), 617–626 (in Chinese with English abstract).
Liu, H.M., Wei, G.L., Xu, Z., Liu, P., Li, Y., 2016b. Quantitative analysis of Fe and Co in Co-substituted magnetite using XPS: the application of non-linear least squares fitting (NLLSF). Appl. Surf. Sci. 389, 438–446.
Lu, Y.Q., Wang, R.C., Lu, X.C., Li, J., Wang, T.T., 2016. Reprint of Genesis of halloysite from the weathering of muscovite: Insights from microscopic observations of a weathered granite in the Gaoling Area, Jingdezhen, China. Appl. Clay Sci. 119, 59–66.
Matusik, J., 2016. Halloysite for adsorption and pollution remediation. In: Yuan, P., Thill, A., Bergaya, F. (Eds.), Nanosized Tubular Clay Minerals. Elsevier, Amsterdam.
McLellan, B.C., Corder, G.D., Ali, S.H., 2013. Sustainability of rare earths-an overview of the state of knowledge. Minerals 3, 304–317.
Mercier, F., Alliot, C., Bion, L., Thromat, N., Toulhoat, P., 2006. XPS study of Eu(III) coordination compounds: core levels binding energies in solid mixed-oxo-compounds EumXxOy. J. Electron Spectros. Relat. Phenom. 150 (1), 21–26.
Miller, S.E., Heath, G.R., Gonzalez, R.D., 1982. Effects of temprerature on the sorption of lanthanides by montmorillonite. Clay Clay Min. 30, 111–122.
Moldoveanu, G.A., Papangelakis, V.G., 2012. Recovery of rare earth elements adsorbed on clay minerals: I. Desorption mechanism. Hydrometallurgy 117–118, 71–78.
Moldoveanu, G.A., Papangelakis, V.G., 2013. Recovery of rare earth elements adsorbed on clay minerals: II. Leaching with ammonium sulfate. Hydrometallurgy 131–132, 158–166.
Nesbitt, H.W., 1979. Mobility and fractionation of rare-earth elements during weathering of a granodiorite. Nature 279, 206–210.
Ng, C., Losso, J.N., Marshall, W.E., Rao, R.M., 2002. Freundlich adsorption isotherms of agricultural by-product-based powdered activated carbons in a geosmin-water system. Bioresour. Technol. 85, 131–135.
Ram, R., Becker, M., Brugger, J., Etschmann, B., Burcher-Jones, C., Howard, D., Kooyman, P.J., Petersen, J., 2019. Characterisation of a rare earth element- and zirconium-bearing ion-adsorption clay deposit in Madagascar. Chem. Geol. 522, 93–107.
Sanematsu, K., Watanabe, Y., 2016. Characteristics and genesis of ion adsorption-type rare earth element deposits. In: Verplanck, P.L., Hitzman, M.W. (Eds.), Rare Earth and Critical Elements in Ore Deposits. Society of Economic Geologists, pp. 55–80.
Schoonheydt, R.A., Johnston, C.T., 2013. Surface and interface chemistry of clay minerals. In: Bergaya, F., Lagaly, G. (Eds.), Handbook of Clay Science, Elsevier, vol. 5, pp. 139–172.
Singh, B., 1996. Why does halloysite roll? – a new model. Clay Clay Miner. 44 (2), 191–196.
Su, W., 2009. Economic and Policy Analysis of China's Rare Earth Industry (in Chinese). Beijing.
Takahashi, Y., Tada, A., Kimura, T., Shimizu, H., 2000. Formation of outer- and inner-sphere complexes of lanthanide elements at montmorillonite-water interface. Chem. Lett. 700–701.
Tanaka, K., Takahashi, Y., Shimizu, H., 2008. Local structure of Y and Ho in calcite and its relevance to Y fractionation from Ho in partitioning between calcite and aqueous solution. Chem. Geol. 248, 104–113.
Tertre, E., Berger, G., Simoni, E., Castet, S., Giffaut, E., Loubet, M., Catalette, H., 2006. Europium retention onto clay minerals from 25 to 150°C: Experimental measurements, spectroscopic features and sorption modelling. Geochim. Cosmochim. Acta 70, 4563–4578.
Tian, J., Chi, R.A., Yin, J.Q., 2010. Leaching process of rare earths from weathered crust elution-deposited rare earth ore. Trans. Nonferrous Met. Soc. China 20 (5), 892–896.
Wang, X.X., Sun, Y.B., Alsaedi, A., Hayat, T., Wang, X.K., 2015. Interaction mechanism of Eu(III) with MX-80 bentonite studied by batch, TRLFS and kinetic desorption techniques. Chem. Eng. J. 264, 570–576.
Xiao, Y.F., Feng, Z.Y., Huang, X.W., Huang, L., Chen, Y.Y., Wang, L.S., Long, Z.Q., 2015. Recovery of rare earths from weathered crust elution-deposited rare earth ore without ammonia-nitrogen pollution: I. leaching with magnesium sulfate. Hydrometallurgy 153, 58–65.

Xiao, Y.F., Feng, Z.Y., Hu, G.H., Huang, L., Huang, X.W., Chen, Y.Y., Long, Z.Q., 2016. Reduction leaching of rare earth from ion-adsorption type rare earths ore with ferrous sulfate. J. Rare Earths 34 (9), 917–923.

Xiao, Y.F., Lai, F.G., Huang, L., Feng, Z.Y., Long, Z.Q., 2017. Reduction leaching of rare earth from ion-adsorption type rare earths ore: II. Compound leaching. Hydrometallurgy 173, 1–8.

Yamaguchi, A., Honda, T., Tanaka, M., Tanaka, K., Takahashi, Y., 2018. Discovery of ion-adsorption type deposits of rare earth elements (REE) in Southwest Japan with speciation of REE by extended X-ray absorption fine structure spectroscopy. Geochem. J. 52, 415–425.

Yang, Z.M., 1987. A study on clay minerals from the REE-rich weathered crust developed on the Longnan granite in Jiangxi. Sci. Geol. Sin. 70–80 (in Chinese with English abstract).

Yang, M.J., Liang, X.L., Ma, L.Y., Huang, J., He, H.P., Zhu, J.X., 2019. Adsorption of REEs on kaolinite and halloysite: a link to the REE distribution on clays in the weathering crust of granite. Chem. Geol. 525 (20), 210–217.

Yin, X.M., Wang, Y.X., Bai, X.J., Wang, Y.M., Chen, L.H., Xiao, C.L., Diwu, J., Du, S.Y., Chai, Z.F., Albrecht-Schmitt, T.E., Wang, S., 2017. Rare earth separations by selective borate crystallization. Nat. Commun. 8, 8.

Yuan, P., Southon, P.D., Liu, Z.W., Green, M.E.R., Hook, J.M., Antill, S.J., Kepert, C.J., 2008. Functionalization of halloysite clay nanotubes by grafting with gamma-aminopropyltriethoxysilane. J. Phys. Chem. C 112, 15742–15751.

Yuan, P., Tan, D.Y., Annabi-Bergaya, F., 2015. Properties and applications of halloysite nanotubes: recent research advances and future prospects. Appl. Clay Sci. 112, 75–93.

Zhang, Q.Q., Sun, J.C., Liu, J.T., Huang, G.X., Lu, C., Zhang, Y.X., 2015. Driving mechanism and sources of groundwater nitrate contamination in the rapidly urbanized region of South China. J. Contam. Hydrol. 182, 221–230.

Zhou, J., Yuan, P., Yu, L., Liu, X., Zhang, B., Fan, W., Liu, D., 2018. Mineralogical characteristics of fine particles of the tuff weathering crust from the Bachi rare earth element (REE) deposit. Acta Mineral. Sin. 38, 420–428 (in Chinese with English abstract).